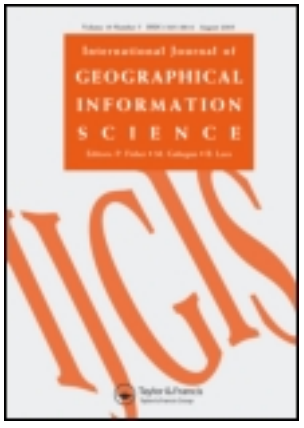

International Journal of Geographical Information Science

Publication details, including instructions for authors and subscription information:
http://www.tandfonline.com/loi/tgis20

Hybrid object-based approach for land use/land cover mapping using high spatial resolution imagery

Eva Savina Malinverni [a], Anna Nora Tassetti [a], Adriano Mancini [b], Primo Zingaretti [b], Emanuele Frontoni [b] & Annamaria Bernardini [a]

[a] Faculty of Engineering - D.A.R.D.U.S. (Dipartimento di Architettura, Rilievo, Disegno, Urbanistica e Storia), Università Politecnica delle Marche, Ancona, Italy

[b] Faculty of Engineering - D.I.I.G.A. (Dipartimento di Ingegneria Informatica, Gestionale e dell'Automazione), Università Politecnica delle Marche, Ancona, Italy

Available online: 19 Jul 2011

To cite this article: Eva Savina Malinverni, Anna Nora Tassetti, Adriano Mancini, Primo Zingaretti, Emanuele Frontoni & Annamaria Bernardini (2011): Hybrid object-based approach for land use/land cover mapping using high spatial resolution imagery, International Journal of Geographical Information Science, 25:6, 1025-1043

To link to this article: http://dx.doi.org/10.1080/13658816.2011.566569

International Journal of Geographical Information Science
Vol. 25, No. 6, June 2011, 1025–1043

Hybrid object-based approach for land use/land cover mapping using high spatial resolution imagery

Eva Savina Malinverni[a]*, Anna Nora Tassetti[a], Adriano Mancini[b], Primo Zingaretti[b], Emanuele Frontoni[b] and Annamaria Bernardini[a]

[a]*Faculty of Engineering – D.A.R.D.U.S. (Dipartimento di Architettura, Rilievo, Disegno, Urbanistica e Storial), Università Politecnica delle Marche, Ancona, Italy;* [b]*Faculty of Engineering – D.I.I.G.A. (Dipartimento di Ingegneria Informatica, Gestionale e dell'Automazione), Università Politecnica delle Marche, Ancona, Italy*

(*Received 10 August 2009; final version received 23 February 2011*)

Traditionally, remote sensing has employed pixel-based classification techniques to deal with land use/land cover (LULC) studies. Generally, pixel-based approaches have been proven to work well with low spatial resolution imagery (e.g. Landsat or System Pour L'Observation de la Terre sensors). Now, however, commercially available high spatial resolution images (e.g. aerial Leica ADS40 and Vexcel UltraCam sensors, and satellite IKONOS, Quickbird, GeoEye and WorldView sensors) can be problematic for pixel-based analysis due to their tendency to oversample the scene. This is driving research towards object-based approaches. This article proposes a hybrid classification method with the aim of incorporating the advantages of supervised pixel-based classification into object-based approaches. The method has been developed for medium-scale (1:10,000) LULC mapping using ADS40 imagery with 1 m ground sampling distance. First, spatial information is incorporated into a pixel-based classification (AdaBoost classifier) by means of additional texture features (Haralick, Gabor, Law features), which can be selected '*ad hoc*' according to optimal training samples ('Relief-F' approach, Mahalanobis distances). Then a rule-based approach sorts segmented regions into thematic CORINE Land Cover classes in terms of membership class percentages (a modified Winner-Takes-All approach) and shape parameters. Finally, ancillary data (roads, rivers, etc.) are exploited to increase classification accuracy. The experimental results show that the proposed hybrid approach allows the extraction of more LULC classes than conventional pixel-based methods, while improving classification accuracy considerably. A second contribution of this article is the assessment of classification reliability by implementing a stability map, in addition to confusion matrices.

Keywords: hybrid classification; texture; LULC; CORINE Land Cover; ADS40; stability map

1. Introduction

Land cover is a fundamental environmental variable for understanding causes and trends of human and natural processes and, consequently, for supporting effective environmental management and monitoring. Qualitative and quantitative information on existing land use is essential for organizations that have to deal with land management decisions, such as government agencies and research institutions.

*Corresponding author. Email: e.s.malinverni@univpm.it

ISSN 1365-8816 print/ISSN 1362-3087 online

DOI: 10.1080/13658816.2011.566569
http://www.informaworld.com

There are many approaches for land use/land cover (LULC) mapping. Traditional techniques include field survey and conventional aerial photograph interpretation. In the past three decades, high spatial resolution imagery from satellite sensors (IKONOS, Quickbird, etc.) or digital aerial platforms (Leica ADS40 and Vexcel UltraCam, etc.) have provided new opportunities for detailed LULC mapping at very fine scales.

Often, LULC map updating must be carried out on a regular basis, so automatic classification algorithms have become increasingly desirable to reduce the high costs associated with photo-interpretation. However, these automated approaches require sophisticated digital image processing and computer vision techniques, and their performance depends strongly on factors such as remote sensing data quality, landscape complexity, training data collection, classification method, etc. (Lu and Weng 2007, Gao and Mas 2008).

Automatic and semi-automatic LULC classification using multispectral image data can be divided into two major approaches: pixel-based and object/region-based classification (Shackelford and Davis 2003, Sims and Mesev 2007). Pixel-based approaches try to identify the class of each pixel from its multispectral values and/or texture measures computed over a neighbourhood. Object-based approaches operate on sets of pixels (objects/regions) that have been grouped together by an image segmentation technique. Shape characteristics and neighbourhood relationships can also be added to spectral/textural information to aid the classification process. Both approaches have drawbacks: the object-based approach is heavily influenced by the quality of segmentation results, while the pixel-based approach, which can exploit only spectral features, might result in errors when the same land cover type does not have unique spectral characteristics and the same spectral response characterizes various different natural objects. Comparisons between the two approaches (Matinfar *et al*. 2007) show that object-based classification often performs more accurately, in addition to having the advantage of being more readily integratable into vector GIS.

In recent years, several techniques (e.g. fuzzy and neural c1assifiers, stepwise optimization approaches) have been developed that can increase the accuracy of automatic classification. In particular, the integration of object- and pixel-based classification shows great potential for improving classification performance (Shackelford and Davis 2003, Wang *et al*. 2004, Yuan and Bauer 2006). An integration of segmentation techniques and pixel-based classification with the aim of assigning a class to each object or segment (*hybrid approach*) may be more efficacious than traditional approaches when classes are not homogeneous in terms of spectral and textural characteristics.

This article presents a new hybrid approach that takes advantage of spectral/textural values and forms factors and a rule-based system (Zingaretti *et al*. 2009). First, different image data sets are provided to an AdaBoost-supervised classifier to yield pixel-based classification results. These results are then integrated with the segmented map obtained from an object-based classification. This last process is performed using the Winner-Takes-All (WTA) algorithm, as derived from other research fields (Ascani *et al*. 2008). Finally, heterogeneous classes are integrated in a decision rule system, taking into account both percentages of classified pixels (resulting from the pixel-based classification) and additional information, such as context, shape and proximity to a certain land cover type. The proposed automatic classification approach provides quick, GIS-ready, LULC maps from high spatial resolution imagery with higher accuracy than conventional pixel- and object-based methods.

A second major contribution of this article is the incorporation of a stability map in the accuracy assessment process, in addition to use of well-known confusion matrices. This assists the user in recognizing regions where classification output should be further checked before use (Woodcock and Gopal 2000, Stehman *et al*. 2003, Wickham *et al*. 2004).

This article is organized as follows: Section 2 introduces the case study area and the available data sets. Section 3 describes each procedure of the supervised hybrid classification methodology developed for this research: feature set identification and selection, pixel-based classification, image segmentation and object rule-based processing. Section 4 presents the advantages and limitations of the hybrid approach, which also includes analysis of the classification results in comparison to pixel-based classification. Finally, Section 5 concludes.

2. Study site and data sets

This case study refers to an area of approximately 16 km^2 located near the city of Ancona (Italy), comprising both urban and rural environments and with a topography that includes flat areas but also the Conero mountain Natural Park. Figure 1 gives an overview of the study image and its geographic location.

The data set is composed of high-resolution multispectral Leica ADS40 images integrated with ancillary information. The ADS40 imagery is mono-temporal (July 2007) and with four spectral wavebands (red, green, blue and near infrared (NIR)).

For this research the CORINE Land Cover (CLC) standard classification system, which was derived from a European Project (EEA 1994) led by the European Environmental Agency, is used. In particular, this work follows the CLC nomenclature to its second and third level (EEA 2007) and adopts a minimum mapping unit (MMU) of 5 mm × 5 mm, corresponding to 0.25 ha and broadly matching a map scale of 1:10,000 (Knight and Lunetta 2003).

3. Methodology

The proposed hybrid classification schema is presented in Figure 2.

Due to its high image spatial resolution, the ADS40 imagery has limited spectral information and shows a high degree of between-pixel variation. This could lead to problems in class information extraction, especially using pixel-based image classification methods,

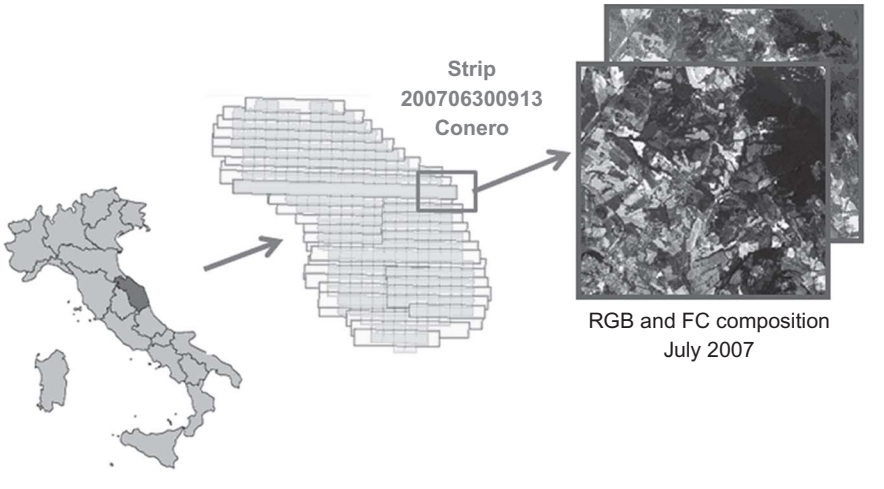

Figure 1. ADS40 strips of the Marche region block (centre) and test imagery (right).

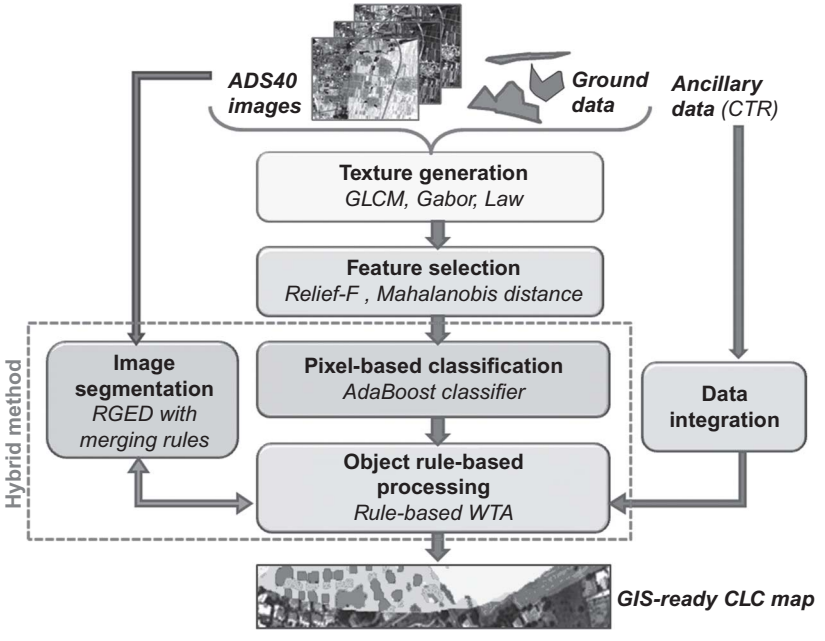

Figure 2. Workflow diagram describing the hybrid classification schema.

in which spatial information existing between a pixel and its neighbours is not used. To overcome these drawbacks and achieve reliable and accurate results, spectral and texture information are initially integrated in the classification schema.

Many parameters influence the generation of texture features, starting with the choice of which ADS40 bands to use for texture analysis. Thirty-three different texture features are generated according to three different texture approaches: the grey-level co-occurrence matrix (GLCM), Gabor-energy and Laws' texture features. The best suited feature set is then chosen by means of the Mahalanobis separability criteria and the Relief-F feature selection algorithm: the 33 texture features are thus reduced to 8.

The selected feature set (8 texture features + 4 ADS40 spectral bands + 1 Normalized Difference Vegetation Index (NDVI) feature = 13 features) is used to run a pixel-based supervised classification with the AdaBoost classifier. These pixels, partitioned into broad categories, form the input to the subsequent object rule-based post-classification processing. In particular, a fuzzy object classifier, implemented on the basis of a WTA approach, is employed to exploit the pixel-based results in classifying objects derived from previous image segmentation, thus providing a refined object classification.

In this hybrid context, image segmentation represents the first step of object-based image analysis and affects the quality of the results directly. The double-headed arrow in Figure 2 points out the possibility of using, in an iterative way, the obtained object-based classification to refine the image segmentation step.

3.1. Texture generation

To avoid increasing feature space dimensionality and redundancy, and due to the strong correlation between some ADS40 spectral bands, only the red and NIR bands are used to

derive texture features since they show the lowest band correlation and the highest variance for the different land cover classes.

The following three feature generation methods were preferred for texture characterization:

- *Grey-level co-occurrence matrix (GLCM) statistical texture features*. The second-order image histogram, referred to as the GLCM of an image, offers much information about inter-pixel relationships and spatial grey-level dependencies. The assumption that no land cover exhibits a preferential directionality is adopted and the grey-scale quantization level is set to 64 to increase computational and statistical performance and to reduce processing time. To avoid generating texture features that are highly correlated with each other, not all texture descriptors derivable from GLCM (Haralick *et al*. 1973) are used. Instead, only four of them are computed for the red and NIR bands and for five window sizes (ranging from 3×3 to 7×7), leading up to the generation of $4\times5=20$ GLCM texture features.
- *Laws' spectral texture features*. Laws' 1D kernels are popular analysis tools for classifying different texture patterns based on regular homogeneity. Twenty-five 2D masks are generated by convolving five 1D kernels (L5, E5, S5, W5 and R5) with each other (Laws 1980). Each of these 1D kernels performs local averaging and edge, spot and wave detection on the sub-image. Only 2 of the 25 generated NIR-texture energy measures are chosen for further analysis, using visual examination. In particular, measures that provide strong discrimination between permanent crops and background are adopted.
- *Gabor Wavelet's spectral texture features*. The Gabor transform reveals the frequency distribution of a signal or an image using a bank of filters. Specifically, the magnitude response is extracted to capture texture homogeneity (Idrissa and Acheroy 2002). The frequency response is Gaussian in shape and the central frequency of each filter was selected to correspond to a peak in the texture power spectrum. The parameters involved are the radial frequency (f), the standard deviation (σ) of the Gaussian curve and the orientation (θ). For the purpose of simplicity, the Gaussian curve is assumed to be symmetrical. The filter bank is created with different orientations (0°, 45°, 90° and 135°), standard deviation ($\sigma=1$) and different frequencies ($f=0.2$, $f=0.5, f=1$). Once the filters are applied, 11 such Gabor magnitudes are extracted.

In short, 33 texture features are generated and selected along with the original four spectral bands (red, green, blue and NIR) and the NDVI band to build the feature set (to the amount of 38 bands) summarized in Table 1.

Table 1. Available feature set (ADS40 spectral bands and texture features).

ID	Band Description
1–4	Multispectral (R-G-B-NIR)
5–12	Haralick NIR
13–24	Haralick Red
25–30	Gabor NIR
31–35	Gabor Red
36–37	Laws NIR

Texture features, differing only by some parameters, are expected to be highly correlated. Using all 38 available features as input and always taking into account their correlation, the Relief-F approach and Mahalanobis measures are carried out for feature selection.

In order to guarantee that each source (spectrum, texture and NDVI) makes the same contribution to the feature space and to avoid scale effects, each source of data is scaled to the same range of grey levels (floating point values from 0 to 1) before running the classification schema. This range is chosen in order to minimize the information loss (especially for the 16-bit spectral data).

3.2. Feature selection

The feature selection is necessary to reduce the feature space dimension and correlation of the generated feature set (a total of 37 plus NDVI). Many approaches are available (Liu and Motoda 2008), mostly aiming to evaluate class separability by means of cost function or metrics (i.e. Jeffrey-Matusita and Mahalanobis distances).

To make a more reliable supervised feature selection, Mahalanobis separability distances, computed for each training class combination, are integrated with other weights coming from the data-mining branch. In particular, the Relief-F algorithm, a modified scheme of the classical Relief (Liu and Motoda 2008), is carried out.

The following parameters are necessary to set up the algorithm: the number n of nearest instances from each class, the maximum distance t_{eq} between two feature values to still consider them equal, the minimum distance t_{diff} between feature values to still consider them different and the sampling parameter m (less than the number M of training instances).

In all the tests n is varied from $n = 1$ to $n = 10$ with $m = M$ while t_{eq} and t_{diff} are calculated according to the following equations:

$$t_{\text{eq}} = \alpha\,(\max(F_i) - \min(F_i)) \quad \alpha = 0.05$$
$$t_{\text{diff}} = \beta\,(\max(F_i) - \min(F_i)) \quad \beta = 0.10$$

where F_i is the ith feature. The values of α and β are set by different simulation runs, according to the literature.

One of the main drawbacks of Relief-F is the computational complexity estimated in $O(mMN)$. To solve the feature selection problem and reduce the computation time (number of training instances over 170,000), the algorithm is executed exploiting a sophisticated computer cluster architecture.

A 2-D matrix *DIS* of size $k \times l$ with $k = (N\,(N-1))/2$ and $l = N$ is generated where N is the feature space dimension. A generic DIS_{ij} element is calculated as the distance between the ith combination (e.g. first combination is represented by classes 1–2, last one by classes *N–1*, *N*) over jth features.

A *minmax* principle is adopted to maximize distances and/or Relief-F weights and minimize band correlation. This principle is implemented by a normalized ranking vector giving more priority to the distance maximization.

A subset of 13 bands was selected for the classification stage.

3.3. Pixel-based classification: AdaBoost classifier

After selecting the feature set to process, a supervised classification is performed by means of the Adaptive Boosting classifier (often known as AdaBoost) which iteratively focuses

on difficult patterns increasing the weights of misclassified training patterns (Sutton 2005). The first problem formulation (Schapire and Singer 1999) is extended in this work using the Real AdaBoost boosting variant to create a strong hypothesis from weak classifiers' combinations and the One Against All technique to obtain a multiclass classification.

One Against All technique works as follows: given C discrete classes (e.g. the CLC codes), the multiclass problem is decomposed into C binary problems to be solved with the Real AdaBoost. A class C is assigned to a given pattern x if it has the greatest positive value, while in case of all negative weights the sample is considered unclassified. However, it is possible to avoid this behaviour choosing the minimum of all negative values.

In order to eliminate 'salt and pepper' noise due to the intrinsic spectral variability characterizing the images, the pixel-based classified output is post-processed by means of 'smoothing' techniques to improve the spatial coherency of pixel-based classifications taking into account the spatial context. In particular, techniques of majority analysis, sieving and clumping are carried out before proceeding with the rule-based object processing.

In this article a Classification And Regression Tree was adopted as a weak learner (Breiman *et al*. 1984, Friedman and Tibshirani 2000); the number (T) of iterations was set at 35 according to a series of simulation runs that evidenced overfitting with $T > 35$.

3.4. Ancillary data integration

In order to improve classification results from image analysis, it is important to be able to integrate ancillary geographical knowledge in the overall classification system. In this research, buildings, roads and rivers can be extracted from the regional technical map and added to the pixel-based classification by means of a raster operation implemented in a stand-alone code (C++ working environment). It is instrumental in the pixel-based classification refinement and especially in preparation for the following object rule-based processing.

3.5. Image segmentation: region growing and edge detection with merging rules

Accurate and precise segmentation is a prerequisite for extracting a set of meaningful objects, such as regions with closed contours (polygons), useful for thematic mapping. The developed segmentation algorithm (Figure 3), derived from Yu and Wang (1999), uses the ADS40 imagery as an input and is based on an image pyramid combining edge-detection (difference in strength, Sobel, Scharr, etc.) with region-growing techniques, in order to obtain a segmentation that outlines the real objects localized into the image with small computation time and strong accuracy. Furthermore, the use of edges during the region growing step allows correct recognition of strong region boundaries and assures robustness with respect to the noise inside the regions (e.g. spikes, small trees, canopies). Another great advantage of this algorithm is that the growing process stops when regions reach strong boundaries.

During the segmentation process, it is possible for too many and unrealistically small regions to be extracted, leading to over-segmentation. To overcome this problem, a redistribution process is then carried out on the basis of specific spectral and spatial parameters (i.e. compactness, convexity) in order to increase the degree of connectivity between adjacent regions. Starting from regions with an area less than the MMU, neighbouring regions with the same characteristics are grouped together to form new regions.

It is important to realize the proper set of working parameters in order to make the algorithm as efficient as possible (Tabb and Ahuja 1997). In particular, the developed segmentation algorithm takes into account compactness, convexity, solidity and roundness

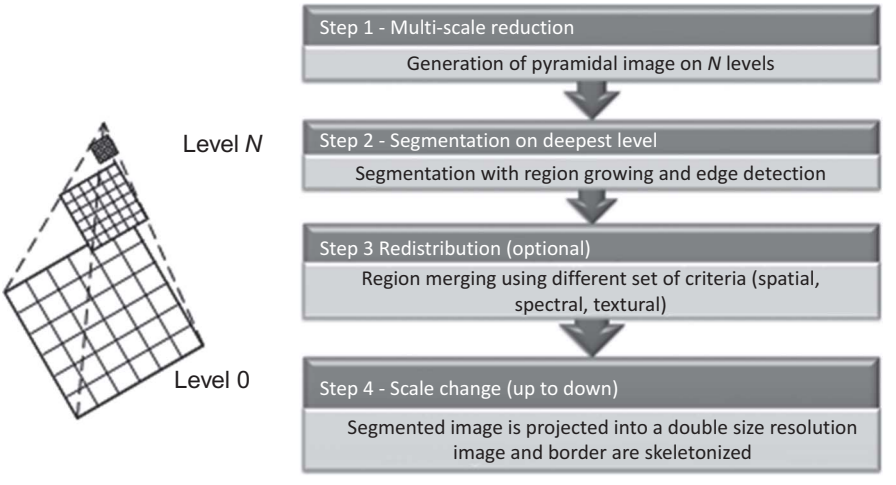

Figure 3. Region growing and edge detection segmentation workflow.

parameters after having investigated them through several tests with different images and pyramid levels.

Finally, selecting a proper set of these parameters and the useful input image (single band, ratio or principal component image), a vector file is produced containing all the information characterizing the regions (Zingaretti *et al*. 1998). A sample of the attribute values resulting from the segmentation process is shown in Figure 4. At this stage, land cover class assignment is not yet achieved.

3.6. Object rule-based processing: a modified Winner-Takes-All approach

Object rule-based processing is performed to improve the pixel-based classification result in terms of spatial consistency, semantic representation and number of extracted classes. In particular, the pixel-based classification is combined with the segmentation result through the overlay technique and the WTA approach, providing meaningful and realistic GIS-ready objects.

FID	Shape	ID	Area	Perimeter	Compactnes	Convexity	Solidity	Roundness	FormFactor	Elongation	RectFit
0	Polygon	1	2957	247	0,24842	0,83806	0,82162	0,70651	0,60907	1,12308	0,62318
1	Polygon	2	4778	386	0,20206	0,81347	0,69987	0,36558	0,40298	1,95455	0,56119
2	Polygon	3	95324	1394	0,24992	0,87303	0,85275	0,63847	0,61643	1,21788	0,61071
3	Polygon	4	3219	303	0,21129	0,78878	0,65215	0,32673	0,4406	1,96491	0,50423
4	Polygon	5	18625	638	0,24137	0,84483	0,87008	0,55343	0,575	1,27778	0,55541
5	Polygon	6	3062	251	0,24876	0,96016	0,8482	0,3108	0,61076	2,19608	0,53606
6	Polygon	7	5776	352	0,24363	0,88636	0,7594	0,34979	0,5858	2,07143	0,56906
7	Polygon	8	3425	282	0,23417	0,95035	0,88777	0,28361	0,54122	3,26316	0,72687
8	Polygon	9	3020	241	0,2573	0,92531	0,82921	0,40867	0,6534	1,94	0,62268
9	Polygon	10	3724	303	0,22726	0,82508	0,73889	0,30837	0,50972	2,25455	0,54604
10	Polygon	11	7084	409	0,2322	0,82885	0,8201	0,429	0,53216	1,76829	0,59579
11	Polygon	12	9097	422	0,25503	0,8981	0,88639	0,6548	0,64192	1,17699	0,6053
12	Polygon	13	3252	324	0,1986	0,76543	0,64383	0,3186	0,38929	1,75385	0,43887
13	Polygon	14	12158	449	0,2771	0,94655	0,92386	0,5294	0,75784	1,76289	0,73298
14	Polygon	15	77292	1337	0,23463	0,79806	0,86944	0,58543	0,54335	1,46429	0,67328
15	Polygon	16	2681	365	0,16007	0,80274	0,47884	0,14027	0,25288	3,05882	0,33698
16	Polygon	17	10386	493	0,23326	0,89858	0,76133	0,32732	0,53699	1,97059	0,50658
17	Polygon	18	18128	590	0,2575	0,93898	0,93724	0,33117	0,65442	2,61386	0,67987
18	Polygon	19	2600	347	0,16581	0,79539	0,58244	0,30027	0,27135	1,64063	0,3869

Figure 4. Extract of segmentation attributes required for the merging procedure.

The WTA algorithm classifies image segments adopting a voting scheme which assigns the segment to its winner class, counting the pixels classified for each class in a generic region. At the end of the process, for each region the winner w_i and the second s_i are assigned, respectively, to the first two classes collecting the majority of votes. From the ratio of these values comes out the stability/confusion index (*CI*):

$$CI = \frac{s_i}{w_i}$$

A low *CI* value confirms the strong presence of a dominant class, while a high *CI* value highlights mixed polygons that may be unreliable.

Afterwards, the core WTA procedure is improved using other rules to enhance the performance of the object classifier and correctly identify critical regions as heterogeneous areas and discontinuous/continuous urban areas.

3.6.1. Hybrid classification rules to identify the CORINE third level

The necessity to obtain a classification according to CLC nomenclature at the third level requires a rule system aid. This nomenclature is in fact strongly related to the image interpretation process, and, to assign detailed legend levels to complex patterns, complex rules that go beyond simple spectral signature identification are needed. When the spectral response is not homogeneous, spatial information (i.e. geometrical segment attributes coming from the segmentation algorithm including size, shape) and WTA land cover percentage over the segment's area are used to build a new learning system. These context relations identify when a class is 'part of' a different class, providing the opportunity to obtain a multiscale database, strongly related to the segments' quality (MMU setting).

In particular, the approach developed enables the identification of heterogeneous agricultural areas belonging to Class 2.4.2 (Complex cultivation patterns) and the differentiation of the urban fabric class according to its density (Continuous Urban Fabric – 1.1.1 and Discontinuous Urban Fabric – 1.1.2).

The decision rules employed are represented below in their logical expressions:

IF (*conditions*) THEN (*decision class*), where the *conditions* consist of some attribute hypothesis and the *decision class* is the class to which the segment is assigned to.

- **Rule 1:** IF Winner is %Area Class 1.1 and PERC-AREA > 80% THEN Class = 1.1.1 Continuous Urban Fabric
- **Rule 2:** IF Winner is %Area Class 1.1 and PERC-AREA > 40% and < 80% THEN Class = 1.1.2 Discontinuous Urban Fabric
- **Rule 3:** IF Winner is %Area Class 1.1 and Second not Class 2.2. and PERC-AREA < 40% THEN Class = 1.1.2 Discontinuous Urban Fabric
- **Rule 4:** IF Winner is %Area Class 1.1 and Second is Class 2.2 and PERC-AREA Class 1.1 < 40% THEN Class = 2.4.2 Complex cultivation patterns
- **Rule 5:** IF Winner is %Area Class 2.2. and Second is Class 1.1 and PERC-AREA Class 1.1 > 20% THEN Class = 2.4.2 Complex cultivation patterns.

Building density is the main criteria used to label a segment as belonging to the built-up class or to the agricultural class. A cultivated segment (permanent crops) with a built-up presence of at least 40% is labelled as complex cultivation pattern (Class 2.4.2).

In dense urban areas, the land cover class confusion tends to be low. The Continuous Urban Fabric class (Class 1.1.1) is assigned when urban structures and roads occupy more than 80% of the surface area. Misunderstandings can arise only in the case of bare soil with similar spectral responses, but they can be limited by checking the segments' dimensions: the segmentation procedure over urban fabrics gives mostly small regions.

Discrimination between continuous and discontinuous urban fabric is performed by computing houses' and roads' area percentages and setting a threshold (between 40% and 80%) to underline a green areas' presence. As the density of urban objects decreases, confusion arises between urban and other land cover classes (especially crop fields) having a spectral signature similar to the urban fabric: there is in fact no vegetation cover on the fields.

Finally, the appearance of a heterogeneous urban land cover class is closely related to the image spatial resolution. Using high spatial resolution images it is necessary to use a more complex rule system than the fuzzy membership function that can be sufficient for coarse spatial resolution images.

4. Tests and results

The classification results are displayed in Figures 5–8.

After having augmented the multispectral ADS40 bands with the selected texture features the pixel-based classification accuracy is improved and it is reasonably good (Figure 5), even if insufficient in terms of homogeneity. A first improvement, by means of the WTA object classification, is shown in Figure 6 where the 'salt and pepper' noise is overcome and a GIS-ready quality is reached, but to the detriment of the number of CLC

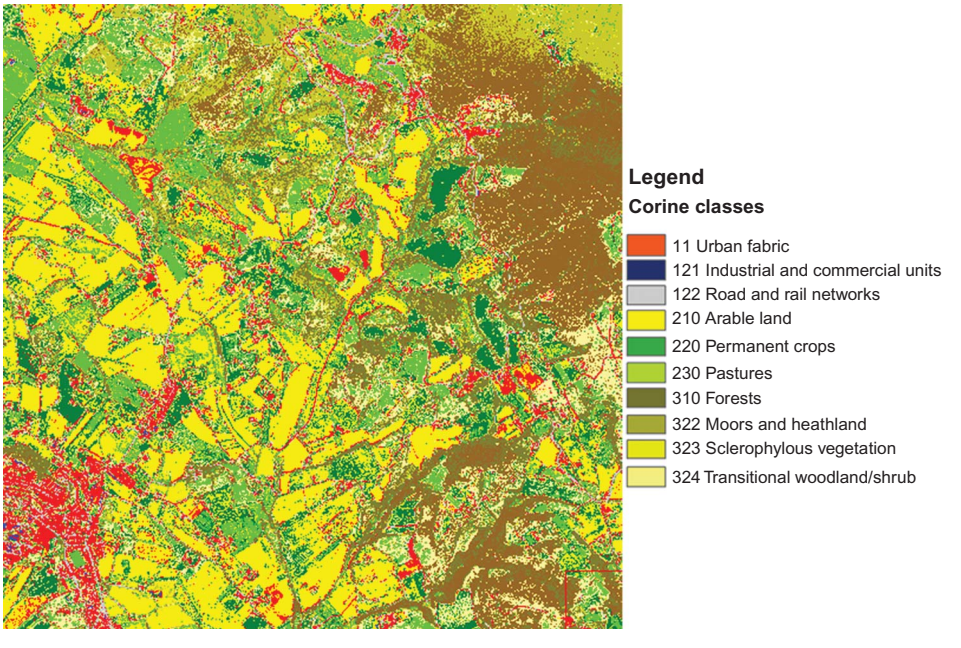

Figure 5. AdaBoost pixel-based classification result and its CLC legend.

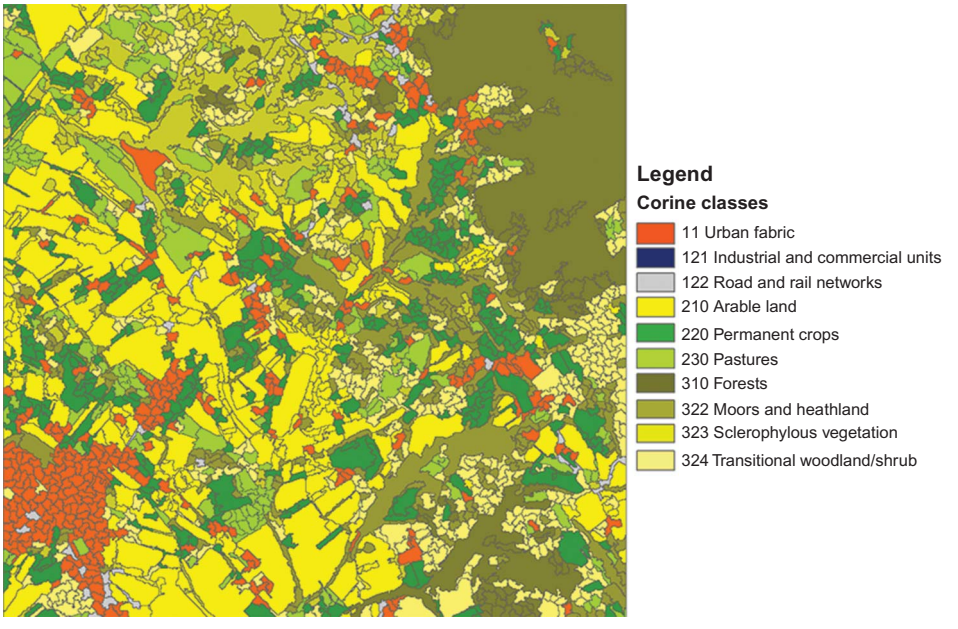

Figure 6. WTA object classification result and its CLC legend.

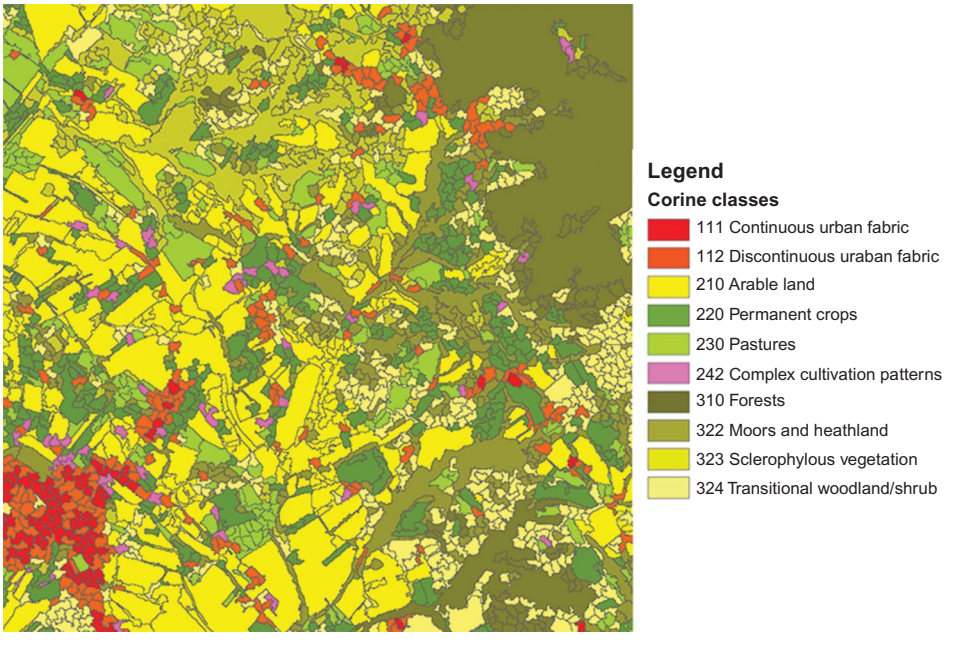

Figure 7. Rule-based WTA classification result and its CLC legend.

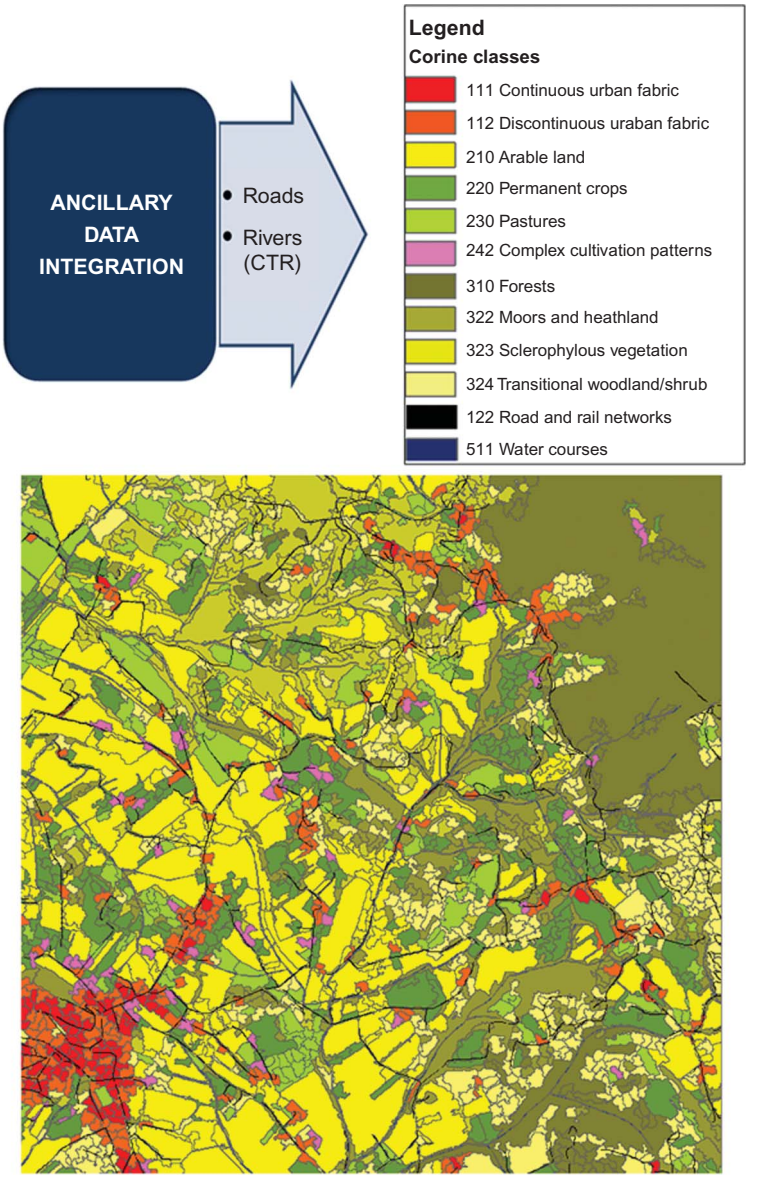

Figure 8. Ancillary data integration and final CLC land use map.

classes extracted: Class 1.2.1 (Industrial and/or Commercial units) disappears because it never wins. Further improvements are shown in Figure 7 where the rule-based WTA approach allows the extraction of Complex cultivation patterns (Class 2.4.2) and distinction between Continuous and Discontinuous Urban Fabric (respectively, Class 1.1.1 and Class 1.1.2).

In order to carry out an unbiased assessment of the accuracy of different approaches, confusion matrices are extracted and the maps derived from classification are compared with a set of control data.

Hereafter in Tables 2 and 3, the developed hybrid classification approach is assessed in comparison with the classic pixel-based approach.

Table 2. AdaBoost pixel-based accuracy assessment.

10 CLC classes				
Feature set:	*SPECTRAL*		*SPECTRAL + TEXTURE*	
Overall accuracy:	74.31%		86.33%	
Kappa coefficient:	0.6737		0.8209	
CLC class	Prod. acc. (%)	User acc. (%)	Prod. acc. (%)	User acc. (%)
110	99.26	82.78	99.46	59.51
121	90.46	99.41	85.21	100
122	98.42	77.75	97.47	83.47
210	55.56	98.14	81.09	99.03
220	83.24	40.94	95.56	54.38
230	75.04	75.42	91.42	85.24
310	82.33	97.72	87.78	98.36
322	77.77	15.56	85.07	18.73
323	83.84	64.67	92.36	69.26
324	57.55	36.35	83.38	58.1

The final rule-based WTA classification produces strong results in terms of overall accuracy (89.02%) and single producer/user accuracy (10 CLC classes with producer accuracy higher than 80%), yielding a legend more detailed than the other classifications.

Table 2 confirms the value of adding texture images in the per-pixel classification approach. By incorporating texture features it is possible to achieve a higher classification accuracy than using only the ADS40 bands: the overall accuracy increases (from 74.31% to 86.33%) and the producer's accuracies for the different classes increase as well.

Lastly, ancillary data integration allows a further refinement of the land use map nomenclature, adding Water courses (Class 5.1.1) and Road and rail networks (Class 1.2.2). Visual inspection of the final CLC map (Figure 8) confirms that the results of this automatic developed classification schema are reasonably strong.

4.1. Stability assessment

The accuracy assessment shown above simply assures that, for example, the pixel-based classification can be considered correct at 86%, but does not identify where regions are located correctly or incorrectly throughout the data set. In this context, the proposed hybrid classification schema provides a stability map, coming from the CI, to distinguish stable segments from unstable ones. Unstable segments are useful in two ways when providing guidance to the user for LCLU map consultation. First, they can help identify where it is necessary to verify manually the output classification map before delivery to end-users. Second, they can highlight class heterogeneity, which is helpful for identification of mixed and complex CLC classes.

The thematic stability map (Figure 9) is obtained using a *CI* threshold of 0.65 and a minimum dominant class threshold of 40%. In Figure 9, red polygons are unstable ($CI >$ 0.65), and yellow ones are stable and cover 86% of the total study area.

The mean stability value of each class is an effective way of illustrating classification accuracy and underlines which classes require careful consideration or further analysis (Figure 10, Table 4).

Table 3. Object classification accuracy assessment: (a) WTA and (b) rule-based WTA.

WTA classification				
8 CLC classes (121 and 122 never win)				
Overall accuracy:			89.41%	
Kappa coefficient:			0.8134	
CLC class	Commission (%)	Omission (%)	Prod. acc. (%)	User acc. (%)
110	4.9	0	100	95.1
210	1.21	9.4	90.6	98.79
220	40.68	19.3	80.7	59.32
230	3.52	9.38	90.62	96.48
310	0	14.47	85.53	100
322	69.24	1.13	98.87	30.76
323	23.12	17.88	82.12	76.88
324	72.4	12.98	87.02	27.6
Rule-based WTA classification				
10 CLC classes (classification refinement: 111, 112 and 242)				
Overall accuracy:			89.0296	
Kappa coefficient:			0.8098	
CLC class	Commission (%)	Omission (%)	Prod. acc. (%)	User acc. (%)
111	0	0	100	100
112	11.73	0	100	88.27
210	1.21	9.4	90.6	98.79
220	41.14	19.32	80.68	58.85
230	3.52	9.38	90.62	95.48
242	0.31	45.75	54.25	99.69
310	0	14.47	85.53	100
322	71.58	1.13	98.87	28.42
323	23.9	17.88	82.12	76.1
324	74.09	12.98	87.02	25.91

While the *CI* quantifies local characteristics, a global stability index (*GSI*) can be computed for every region (R_i) to provide a global overview:

$$GSI = \sum_{i=1}^{N} \left(\frac{\mathrm{St}\,(R_i)}{\mathrm{Area}\,(R_i)} \right)$$

$$\mathrm{St}\,(R_i) = \begin{cases} \mathrm{Area}(R_i) & \text{if } CI \leq TH \\ 0 & \text{if } CI > TH \end{cases}$$

A parametric analysis of the *GSI* trend for every class is shown in Figure 11.

Further checking is performed by overlaying the stability map and the control data set (Figure 12). In Figure 12, red segments identify control data that are generally inaccurately predicted in the rule-based WTA classification. About 90% of the control data are shown

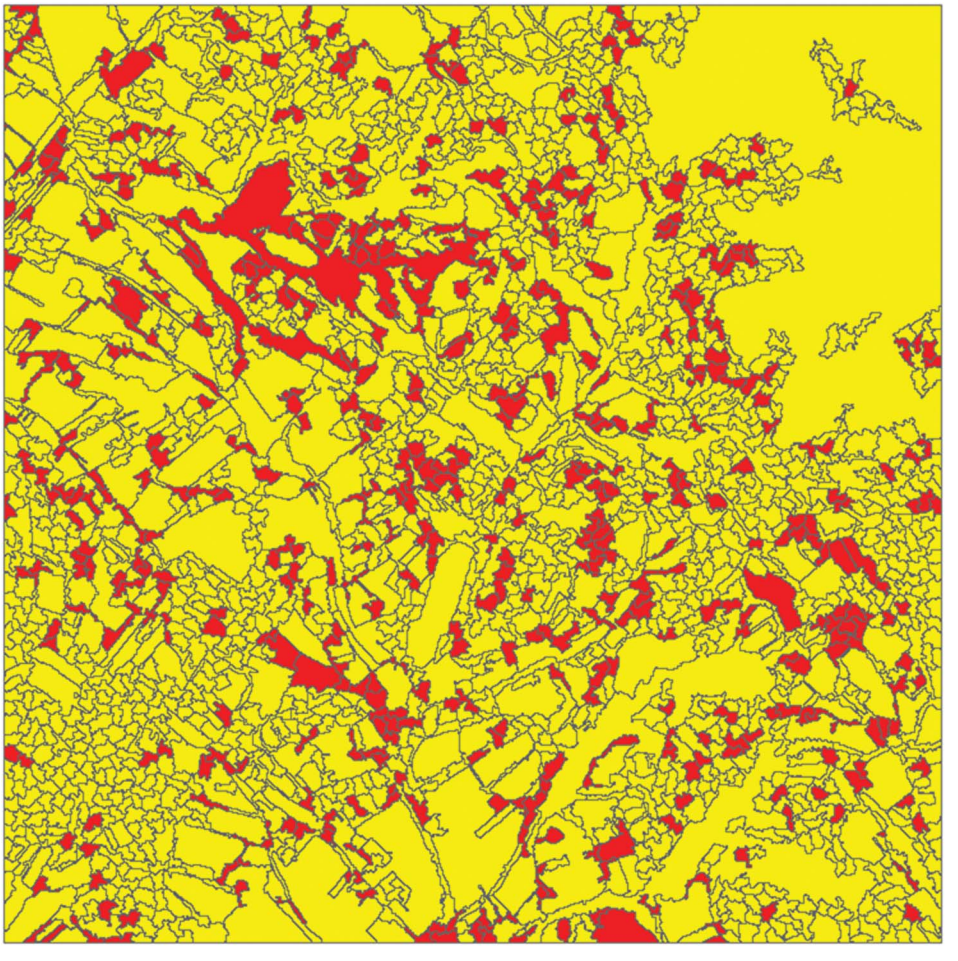

Figure 9. Stability map – rule-based WTA classification: yellow polygons are stable (86% of area), while red ones are unstable (14% of area).

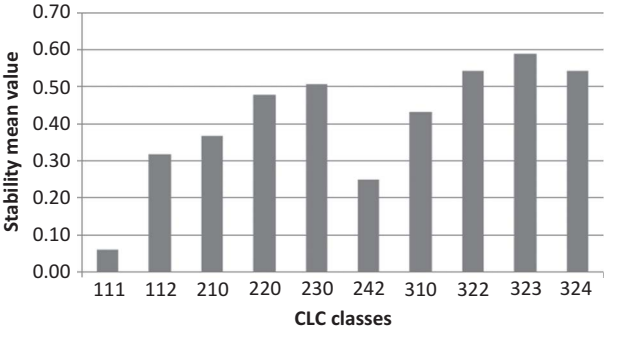

Figure 10. Mean stability value for each CLC class.

Table 4. Class Stability.

CORINE classes	Stability (S)
1.1.1	100%
1.1.2	91%
2.1.0	84%
2.2.0	76%
2.3.0	74%
2.4.2	100%
3.1.0	88%
3.2.2	69%
3.2.3	68%
3.2.4	75%

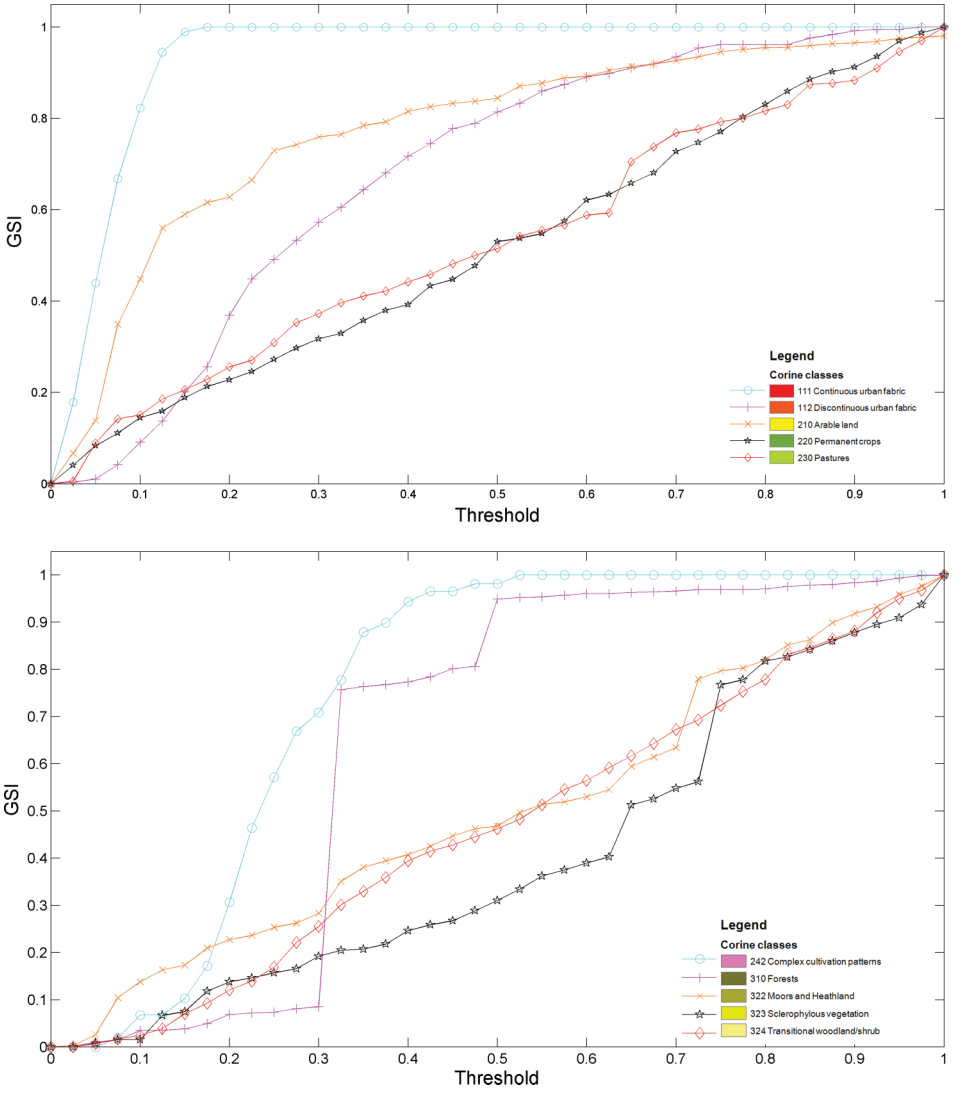

Figure 11. Trend of global stability index for each CLC class.

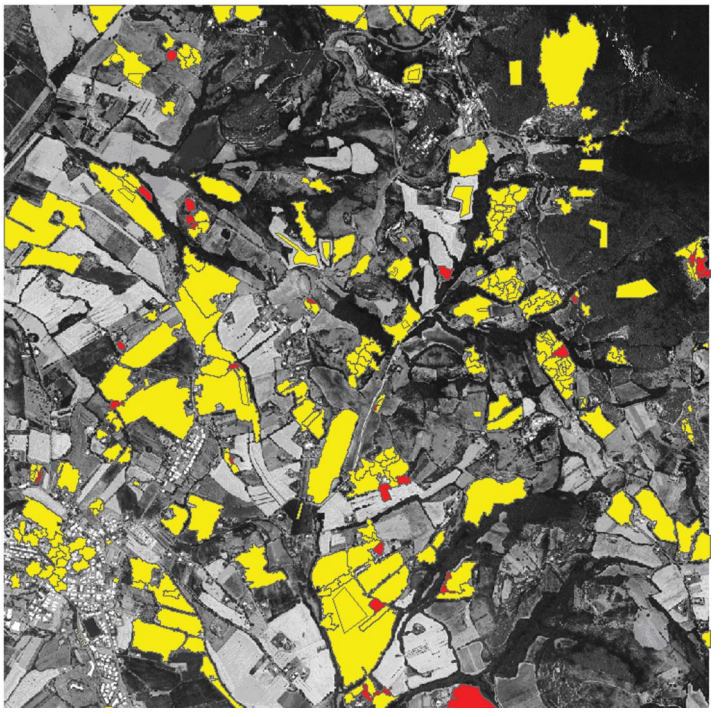

Figure 12. Overlay of stability map and control data set.

to be stable, and this corresponds with the overall accuracy of the rule-based WTA map compared against the control data set. The unstable regions in great part belong to the heterogeneous class, which is relatively inaccurate in general (maximum accuracy of 54% in Table 3). It is clear that additional rules and supplementary information are necessary to avoid misclassification.

5. Conclusions

In this article, a new method for high spatial resolution image classification is proposed. This integrates a pixel-based classification method (AdaBoost classifier) with an object-based classification method, based on a WTA system augmented with rules.

The classification output shows a LCLU map with 12 classes (CLC second and third level). Classification accuracy is improved through various procedures. First, the per-pixel classification accuracy increases from 74.31% to 86.33% by including texture analysis in the classification schema. Then, object-based WTA classification removes noise (misclassified pixels) from the result and accuracy increases further to 89.41%. A refinement is implemented by means of a rule-based WTA approach that allows the extraction of new third-level CLC classes and achieves an accuracy of 89.02% by cross-reference with a different object-based control data set. Figure 13 shows the control data set used for the pixel-based accuracy assessment and the more exhaustive control data set derived by photo-interpretation of the segmented image used for object-based accuracy assessment.

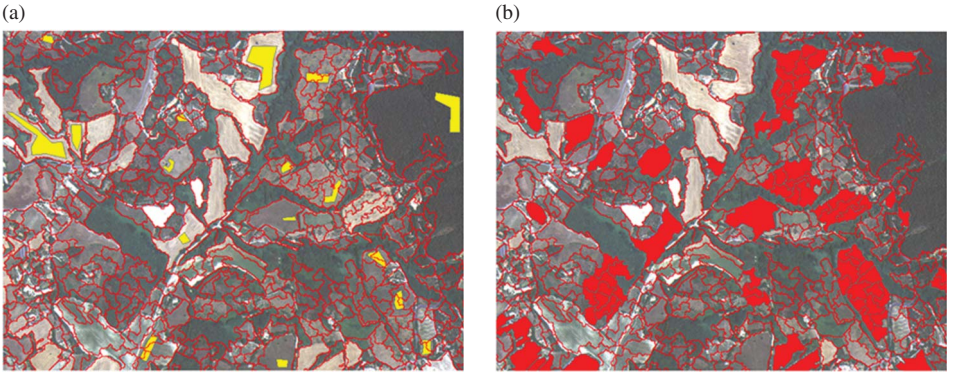

Figure 13. (a) Pixel-based and (b) object-based ground control data.

A final output of the research is a stability map that helps the user distinguish stable and unstable regions, whereby unstable regions can be further verified before use of the final classification product. This is an efficient checking procedure, targeting only those locations that have a relatively high likelihood of misclassification.

The proposed method provides accurate results that can be used for a range of applications and by a range of users (i.e. urban planner, environmental agencies). Moreover, the final product is a GIS-ready map that can easily supplement and enhance other thematic databases.

References

Ascani, A., Frontoni, E., Mancini, A. and Zingaretti, P., 2008. Feature group matching for appearance-based localization. *In*: *International conference on intelligent robots and systems* IROS 2008 Nice. 3933–3938.

Breiman, L., *et al*., 1984. *Classification and regression trees*. Pacific Grove, CA: Wadsworth.

European Environment Agency (EEA)., 1994. *CORINE land cover – part 1: methodology*. Available from: http://www.eea.europa.eu/publications/COR0-part1 [Accessed 10 October 2010].

European Environment Agency (EEA)., 2007. *CLC2006 technical guidelines - Technical report*. Available from: http://www.eea.europa.eu/publications/technical_report_2007_17 [Accessed 10 October 2010].

Friedman, T.H. and Tibshirani, R., 2000. Additive logistic regression: a statistical view of boosting. *The Annals of Statistics*, 38 (2), 337–374.

Gao, Y. and Mas, J.F., 2008. A comparison of the performance of pixel based and object based classifications over images with various spatial resolution. *On Line Journal of Earth Science*, 2, 27–35.

Haralick, R., Shanmugam, K., and Dinstein, I., 1973. Texture features for image classification. *IEEE Transactions on Systems, Man, and Cibernetics*, Smc-3, 610–621.

Idrissa, M. and Acheroy, M., 2002. Texture classification using Gabor filters. *Pattern Recognition Letters*, 23, 1095–1102.

Knight, J.F. and Lunetta, R.S., 2003. An experimental assessment of minimum mapping unit size. *IEEE Transactions on Geoscience and Remote Sensing*, 41, 9.

Laws, K.I., 1980. *Textured image segmentation*. Dissertation (PhD). University of Southern California.

Liu, H. and Motoda, H., 2008. *Computational methods of feature selection*. Boca Raton, FL: Chapman and Hall/CRC.

Lu, D. and Weng, Q., 2007. A survey of image classification methods and techniques for improving classification performance. *International Journal of Remote Sensing*, 28 (5), 823–870.

Matinfar, H.R., *et al*., 2007. Comparisons of object-oriented and pixel-based classification of land use/land cover types based on Lansadsat7, Etm+ spectral bands (case study: arid region of Iran). *American-Eurasian Journal of Agricultural & Environment Science*, 2 (4), 448–456.

Schapire, R.E. and Singer, Y., 1999. Improved boosting algorithms using confidence-rated predictions. *Machine Learning*, 37 (3), 297–336.

Shackelford, A.K. and Davis, C.H., 2003. A combined fuzzy pixel-based and object-based approach for classification of high-resolution multispectral data over urban areas. *IEEE Transactions on Geoscience and Remote Sensing*, 41 (10), 2354–2363.

Sims, F.M. and Mesev, V., 2007. Use of ancillary data in object based classification of high resolution satellite data. *In*: *Urban remote sensing joint event*. URBAN 2007 – URS 2007. Paris, 1–10.

Stehman, S.V., *et al*., 2003. Thematic accuracy of the 1992 national land-cover data for the eastern United States: statistical methodology and regional results. *Remote Sensing of Environment*, 86, 500–516.

Sutton, C.D., 2005. Classification and regression trees, bagging, and boosting. In: C.R. Rao, E.J. Wegman and J.L. Solka (Eds), *Handbook of Statistics*. vol. 24. Amsterdam: Elsevier.

Tabb, M. and Ahuja, N., 1997. Multiscale image segmentation by integrated edge and region detection. *IEEE Transactions on Image Processing*, 6 (5), 642–655.

Wang, L., Sousa, W., and Gong, P., 2004. Integration of object-based and pixel-based classification for mangrove mapping with IKONOS imagery. *International Journal of Remote Sensing*, 25 (24), 5655–5668.

Wickham, J.D., *et al*., 2004. Thematic accuracy of the 1992 national land-cover data for the western United States. *Remote Sensing of Environment*, 91, 452–468.

Woodcock, C.E. and Gopal, S., 2000. Fuzzy set theory and thematic maps: accuracy assessment and area estimation. *International Journal of Geographical Information Systems*, 14 (2), 153–172.

Yu, Y.W. and Wang, J.H., 1999. Image segmentation based on region growing and edge detection. *In*: *Proceedings of IEEE international conference on systems, man, and cybernetics*. vol. 6. 798–803.

Yuan, F. and Bauer, M.E., 2006. Mapping impervious surface area using high resolution imagery: a comparison of object-based and per pixel classification. *In*: *Proceedings of ASPRS 2006 annual conference*, Reno, Nevada.

Zingaretti, P., *et al*., 2009. A hybrid approach to land cover classification from multispectral images. In: 15th *International conference on image analysis and processing (ICIAP)*, 8–11 September 2009 Vietri sul Mare, Italy.

Zingaretti, P., Gasparroni, M., and Vecci, L., 1998. Fast chain coding of region boundaries. *IEEE Transactions on Pattern Analysis and Machine Intelligence*, 20 (4), 407–415.